Nuclear Instruments and Methods in Physics Research B 340 (2014) 58–62

Contents lists available at ScienceDirect

Nuclear Instruments and Methods in Physics Research B

journal homepage: www.elsevier.com/locate/nimb

The use of electron Rutherford backscattering to characterize novel electronic materials as illustrated by a case study of sputter-deposited NbO_x films

M. Vos [a,*], X. Liu [b], P.L. Grande [b,c], S.K. Nandi [b,d,e], D.K. Venkatachalam [b], R.G. Elliman [b]

[a] Atomic and Molecular Physics Laboratories, Research School of Physics and Engineering, The Australian National University, Canberra 0200, Australia
[b] Electronic Materials Engineering Department, Research School of Physics and Engineering, The Australian National University, Canberra 0200, Australia
[c] Instituto de Fisica da Universidade Federal do Rio Grande do Sul, Avenida Bento Goncalves 9500, 91501-970 Porto Alegre, RS, Brazil
[d] Research School of Astronomy and Astrophysics, The Australian National University, Canberra, ACT 2611, Australia
[e] Department of Physics, University of Chittagong, Chittagong 4331, Bangladesh

ARTICLE INFO

Article history:
Received 8 February 2014
Received in revised form 6 June 2014
Accepted 24 June 2014
Available online 8 August 2014

Keywords:
Electron Rutherford backscattering
NbO_x
Reactive sputter deposition

ABSTRACT

Electrons scattered over large angles at relatively high energies (40 keV) are used to study NbO_x films. These films were deposited by reactive sputter deposition on a Si substrate using a Nb target and an Ar/O_2 gas mixture. Energy spectra of electrons scattered from such samples exhibit elastic scattering peaks for each component due to the energy difference associated with scattering from different masses. The spectra provide in this way information about the film thickness as well as its stoichiometry. The stoichiometry and the deposition rate depends on the concentration of O_2 in the mixture. For Nb_2O_5-like films the energy loss measurements also give an estimate of the band gap, but for Nb films with lower O concentration the band gap is not resolved. This work illustrates the possibility of characterizing modern transition metal oxide films in a fairly simple electron scattering experiment.

1. Introduction

There is ongoing interest in exploring the physics of novel electronic materials. In particular transition metal oxides with their exotic properties have the potential of forming the basis of nano-scale electronic components with unique properties. Characterizing them in terms of composition, thickness and electronic structure is a mandatory step in their development. Recently electron Rutherford backscattering (ERBS) has presented itself as a candidate for determination of the thickness of the layers (up to ≈50 nm for the overlayer-substrate combination used here) as well as their elemental composition and, when extending the measurement to larger energy losses, their electronic structure. We have demonstrated the capabilities of ERBS for the thickness measurements of HfO_2 films grown by atomic layer deposition [1] (extending even to the isotopic composition of such films [2]), and composition and electronic structure were determined for TaO_x films formed by ion implantation [3].

Here we present similar measurements, but now for NbO_x films grown by sputter deposition. ERBS is the electron analogue of (ion) Rutherford backscattering (RBS). Just like RBS it relies on energy loss due to scattering of incoming particles. The energy transfer in this scattering process is very small for ERBS (typically several eV) but still enough to determine the mass of the scatterer. The energy loss due to electronic excitations presents itself somewhat differently in ERBS and RBS. For RBS the energy loss can be described as a continuous process, for ERBS it is quantized (just as in X-ray photoemission spectroscopy (XPS)) i.e. the energy loss events are separated in space (the mean separation is given by the inelastic mean free path), and the amount of energy loss in each event is given by the loss function, which can be described in terms of the dielectric function of the material.

Nb_2O_5 and NbO_2 are of particular interest in this regard as they respectively exhibit resistive switching and threshold switching characteristics as require for the fabrication of an integrated memory device and selector element. The latter is required for 3-D memory arrays to avoid inadvertent addressing of memory elements due to sneak current paths (as explained e.g. in Ref. [4]) but adding a selector element generally increases the device complexity and hence production costs. A hybrid device based on a Nb_2O_5/NbO_2 bilayer structure could address this issue, with the high resistivity of the NbO_2 layer at low current densities greatly reducing the sneak current, and the Nb_2O_5 layer serving as the

* Corresponding author.
E-mail address: maarten.vos@anu.edu.au (M. Vos).

http://dx.doi.org/10.1016/j.nimb.2014.06.024
0168-583X/

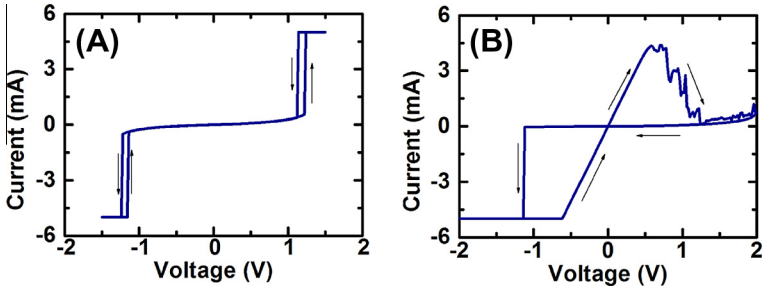

Fig. 1. An example of an I–V curve as measured for (A) a NbO_x film grown using a mixture with $Ar:O_2$ = 18:2 and (B) a film grown using a ratio of $Ar:O_2$ = 16:4. Films were grown on a Pt substrate and a Pt cap was applied later to facilitate the I–V measurements.

memory element [5,6]. Recently, Pickett and coworkers also demonstrated that NbO_2 threshold switching devices can form the active components necessary to build a neuristor, a biomimetic threshold spiking device. This finding makes new applications of NbO_2 threshold switching possible, for example in signal repetition applications, and other neuristor logic devices [7,8].

Threshold switching in NbO_2 is explained by a Joule-heating-induced metal–insulator phase transition which causes a dramatic decrease in resistance. Due to positive feedback (once a small part of the device is Joule heated above the transformation temperature, more current flows through this region heating it further and expanding the conductive region) the transition from a resistive to a conductive state is sudden. The formation of the metallic phase is reversible: it disappears quickly when the device cools down after the removal of the bias. This volatility distinguishes threshold switching from 'memory switching' (found in e.g. Nb_2O_5) where the resistive state is retained indefinitely without static bias. The ability to trigger the insulator–metal transition electrically (by applying small voltages) at or near room temperature offers great potential for novel, low-power oxide electronics in particular for memory selecting elements.

In Fig. 1 we show the I–V characteristics of two NbO_x films, deposited under slightly different conditions. Fig. 1(A) shows characteristics of a film deposited under a low partial pressure of O_2 which exhibits threshold switching behavior, while Fig. 1(B) shows the characteristics of a film deposited under a higher partial pressure of O_2 which shows resistive switching behavior. For the latter case applying a large positive voltage transforms the film to a highly resistive state, whereas applying a large negative voltage results in a highly conductive state. This change in resistivity is attributed to electric-field induced migration of O atoms near the outer NbO_x–Pt interface. The asymmetry is caused by the fact that for this growth procedure the interface that is formed by sputter-deposition of NbO_x on Pt is ohmic, whereas the interface that is formed by evaporating Pt on NbO_x behaves initially as a Schottky diode.

In this paper we demonstrate that ERBS measurements can resolve materials properties that relate to these very different I–V characteristics.

2. Experimental details

ERBS measurements were done with our spectrometer described extensively elsewhere, see e.g. [9,10]. Briefly 40 keV electrons are scattered over 135.5° from a target and the scattered electrons are energy-analysed with a resolution of 0.3 eV. This is good enough to resolve the contribution of the elastic peak of Nb, Si and O. The zero point of the energy scale is not exactly known and we use the energy peak of the heaviest peak (in this case Nb) to fix the zero position by assuming that it has a recoil energy as calculated for an electron scattering from a free atom (0.84 eV for electrons scattering from free Nb under these conditions).

To determine the elemental concentrations we use the elastic scattering cross section as calculated by the ELSEPA package of Salvat and coworkers [11]. The calculated cross section for Si and O are fairly close to the Rutherford cross section, but the Nb cross section exceeds Rutherford by 27% [12].

Thin films of niobium oxide (NbO_x) were deposited on Si substrate using reactive DC magnetron sputtering method from a metallic niobium target at room temperature. Various sub-stoichiometric (NbO_x) and stoichiometric (Nb_2O_5) samples were fabricated. The different stoichiometries were obtained by changing the argon to oxygen mass flow ratio (19/1, 18/2, 16/4, 12/8 at 20 sccm) at a constant total pressure of 4mTorr and constant power of 300 W. The deposition time was fixed at 7.5 min. It was possible to get an estimate of the overlayer thickness by RBS by measuring the area of the Nb peak and calculating the corresponding thickness using the density of Nb in Nb_2O_5. For the measurement of the stoichiometry of the film we can not use RBS as for a NbO_x layer grown on Si the O signal is on a very large Si background. In order to get information about this stoichiometry from RBS we grew a NbO_x layer on carbon. For this deposition the power was only 150 W. A reference sample of (relatively thick) Nb_2O_5 was grown by annealing Nb metal for 30 min at 600 °C in an oxygen atmosphere.

3. Results

In Fig. 2 we show the ERBS spectra as obtained for the film deposited with a high O_2 partial pressure ($Ar:O_2$ = 12:8). Here the deposition rate was low and the thickness was such that Si from the substrate still contributes significantly to the spectrum. Thus we observe 3 peaks, one is separated by ≈2 eV from the first peak, and the second one by ≈4.0 eV. This agrees well with the calculated separation (1.95 and 4.04 eV) for scattering from Nb (main peak) Si (central peak) and O (peak at highest energy loss). Rotating the sample by 35° makes the measurement much more surface sensitive as after rotation the outgoing trajectory is very glancing (80° away from the surface normal). Indeed the central (Si) peak is now greatly reduced. From the peak area ratio of the Nb peak and the Si peak we can calculate the thickness of the overlayer, as explained in Ref. [1]. From the TPP theory [13] (developed for electron energies of several keV, but used here at 40 keV) we deduced an inelastic mean free path for Nb_2O_5 of 41.5 nm and for Si of 53.6 nm. Using these values we calculate for this sample an overlayer thickness of 9 nm. The thickness obtained for the measurements at the two different geometries was the same.

The ratio of the Nb and the O peak area for the sputter deposited film is, within the precision of the measurement, the same as the Nb:O peak area ratio of the thermally grown oxide film for which it is well established that the stoichiometry is Nb_2O_5. Thus the

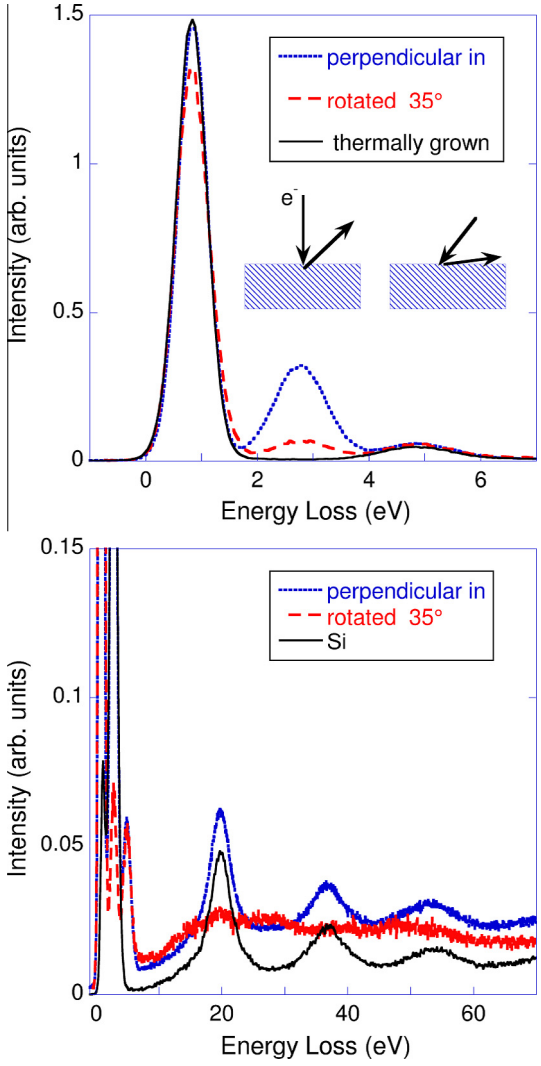

Fig. 2. Spectra of the elastic peak region (top) for the sample deposited at a relatively high O_2 partial pressure as obtained for a bulk (labelled "perpendicular in") and surface sensitive (labelled "rotated 35°") geometry compared to the spectrum of a thick, thermally grown Nb_2O_5 layer. The bottom shows the spectra of the same film on an extended scale, but now compared to the energy loss spectrum of silicon.

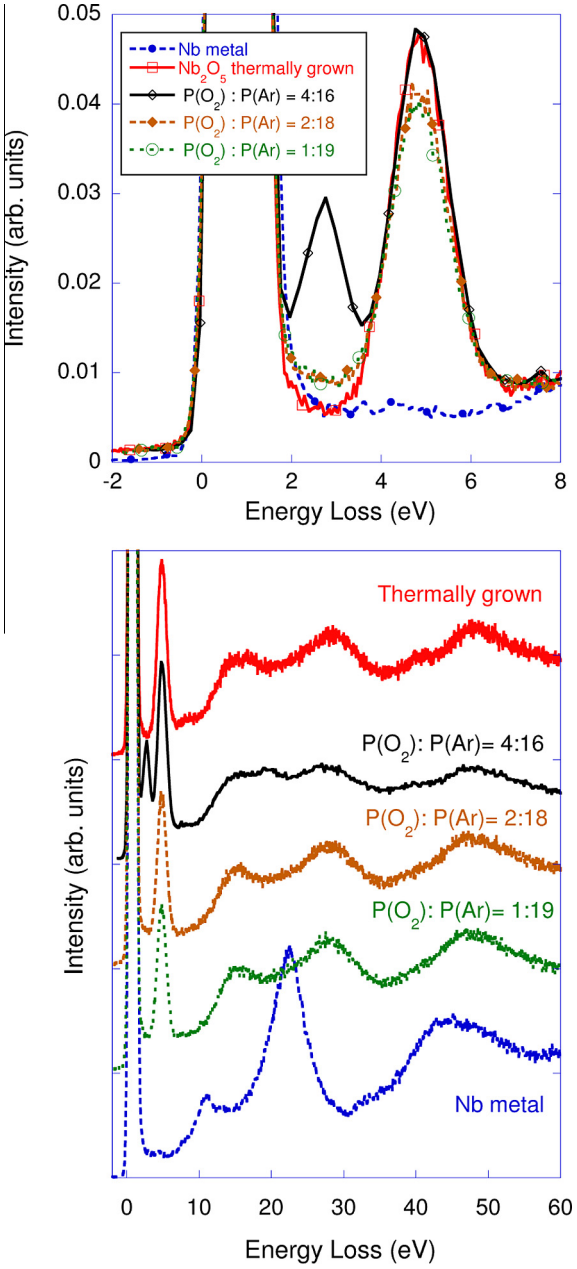

Fig. 3. The top panel shows the elastic peak region of the loss spectra for Nb (metal), thermally grown Nb_2O_5 and 3 spectra of sputter-deposited layers with an O_2 to Ar partial pressure ratio as indicated. The lower panel showing the same spectra over a larger energy loss range. Even for lowest O_2 partial pressures there is no contribution of Nb metal to the energy loss spectrum.

stoichiometry of these sputter-deposited films is also very close to Nb_2O_5. The same conclusion is reached if we analyze the experimental data using the theoretical elastic scattering cross sections of Nb and O [12].

Looking at a wider energy range (lower panel of Fig. 2) we see the contributions from electrons that were deflected from a nucleus *and* created one or more electronic excitations. As explained in Ref. [3] this part of the spectrum originates on average from a somewhat larger depth. In the bulk-sensitive geometry we see now regularly-spaced peaks, just as in the energy loss spectrum of a Si sample without a deposited overlayer which is shown as well. The separation of the Si elastic peak and the plasmon is 17 eV, but the total energy loss is 19 eV (17 eV (plasmon energy) +2 eV (recoil energy for Si) [14]. Thus for this sample the contribution of the substrate dominates the energy loss spectrum. In the glancing geometry the energy loss spectrum has less distinct peaks and is due to both the substrate and the overlayer.

From Fig. 3 (top panel) we see that reducing the O_2 concentration in the Ar:O_2 mixture to 16:4 reduces the Si peak intensity strongly, and this peak is below the detection limit for the deposition with Ar:O_2 mixtures of 18:2 and 19:1, indicating much thicker films in these cases. Clearly the deposition rate increases dramatically with decreasing O_2 concentration. The film thickness for the 16:4 mixture as obtained by ERBS was 39 nm, for the two other mixture only a lower limit of 50 nm can be determined (as no Si peak is visible in the spectrum).

As before the Nb peaks in Fig. 3 were normalized to unit area. Interestingly, now the Nb:O peak area ratio depends on the O_2 partial pressure. For the 4:16 mixture the peak area ratio can still not be distinguished from that of the thermally grown film, but for the lower oxygen concentration the O peak is clearly less intense and the films are sub-stoichiometric (compared to Nb_2O_5). The obtained nominal stoichiometry, as well as the thicknesses are given in table Table 1.

Table 1
Thickness and stoichiometry as obtained by ERBS and RBS. The first column shows the Ar/O_2 pressure ratio of the gas used in the deposition. The second and third column is the thickness and stoichiometry of the deposited layer as determined by ERBS, the last two columns are the same quantities as determined by RBS. Note however, that for the stoichiometry we used a separate sample with the NbO_x layer grown on carbon.

Ar/O_2	T (nm) ERBS	Nb_2O_x (ERBS)	T (nm) RBS	Nb_2O_x (RBS)
19:1	>50	Nb_2O_4	93	$Nb_2O_{4.3}$
18:2	>50	$Nb_2O_{4.3}$	88	–
16:4	39	Nb_2O_5	37	$Nb_2O_{5.5}$
12:8	9	Nb_2O_5	8	$Nb_2O_{5.8}$

In the lower panel of Fig. 3 we show the energy loss spectra of these samples, sputter-deposited at a lower O_2 partial pressure, over a larger loss range, as well as the spectra from thermally grown Nb_2O_5 and Nb metal. The loss spectra of all sputter-deposited films are fairly similar and resemble that of the native oxides. The spectra for the 4:16 mixture still shows a trace of the Si plasmon peak at 19 eV energy loss, consistent with the fact that there the deposited layer is still fairly thin. The Nb metal film has a strong peak near 21 eV. This peak is absent in the sputter-deposited films, so there is no sign of metallic Nb in the sub-stoichiometric films.

Transmission electron energy loss measurements from Bach et al. at 200 keV show subtle differences between the intensity ratio of the different features in the loss spectrum between NbO_2 and Nb_2O_5 [15]. In particular the peak near 15 eV is stronger than the peak near 25 eV for Nb_2O_5 but for NbO_2 it is the other way around. We do not see such differences between thermally grown Nb_2O_5 samples and samples with a stoichiometry close to that of NbO_2. However our spectra are not deconvoluted for multiple scattering (which is not straight forward as we do not know the thickness in all cases) and this can affect the apparent intensity of different peaks in the spectrum.

It is more interesting to focus attention on the 'band gap region'. Here the O elastic peak complicates the interpretation of these data. Therefore we decreased the energy of the incoming beam to 5 keV. The O–Nb splitting is now reduced by a factor of 8 and the Nb and O elastic peaks have merged. The energy loss spectra taken at 5 keV for samples grown with an $Ar:O_2$ pressure ratio of 16:4 and 19:1 are shown in Fig. 4. We aligned the elastic peak with 0 eV energy loss. For the sample grown under high O_2 flux (with a stoichiometry close to Nb_2O_5) the onset of the loss spectrum is near 3.8 eV, a slightly larger value than usually quoted for the band gap of Nb_2O_5 (3.4 eV). For the sample grown under a smaller O_2 flux (with a stoichiometry close to $Nb_2O_{4.3}$) there is an increase of the loss spectrum at a similar energy loss, but there is extra intensity extending all the way from this onset to the elastic peak. This behavior is quite universal, we have observed it as well when comparing sub-stoichiometric and stoichiometric hafnium oxides and tantalum oxides and have been seen in many other REELS experiments, e.g. for the case of the reduction of a TiO_2 surface by sputtering, see Ref. [16]. When the films are prepared in such a way that the cation is not fully oxidized, there appears to be a tail extending from the elastic peak, partially filling in the band gap region seen for the fully oxidized material.

To understand this it is helpful to consider the sketch of the density of states shown in the top half of Fig. 4. For Nb_2O_5 the Nb atoms have a charge of 5^+ (iso-electronic with Kr). The valence band is derived from O 2*p* states, and the valence states derived from $Nb_{4d,5s}$ electrons are empty. Thus the gap observed is a signature of the band gap.

If the cation is not fully oxidized then some of the $Nb_{4d,5s}$ states are occupied, and there are additional excitations possible (shown in red in Fig. 4. These excitations cause the additional, but fairly featureless, intensity in the band gap region of Nb_2O_5. For the case of NbO_2 there is a phase transition. In the low-temperature (high resistance phase) the crystal structure of NbO_2 has dimerized (Peierls transition), enlarging the unit cell and causing a gap at the Fermi level [17]. At high temperatures this dimerization disappears and the material becomes a reasonably good conductor. Unfortunately our energy resolution is not good enough to resolve this dimerization gap (≈1 eV) near the very intense elastic peak. Thus under these conditions the onset of O 2*p* excitations in the EELS spectrum should not be confused with the band gap.

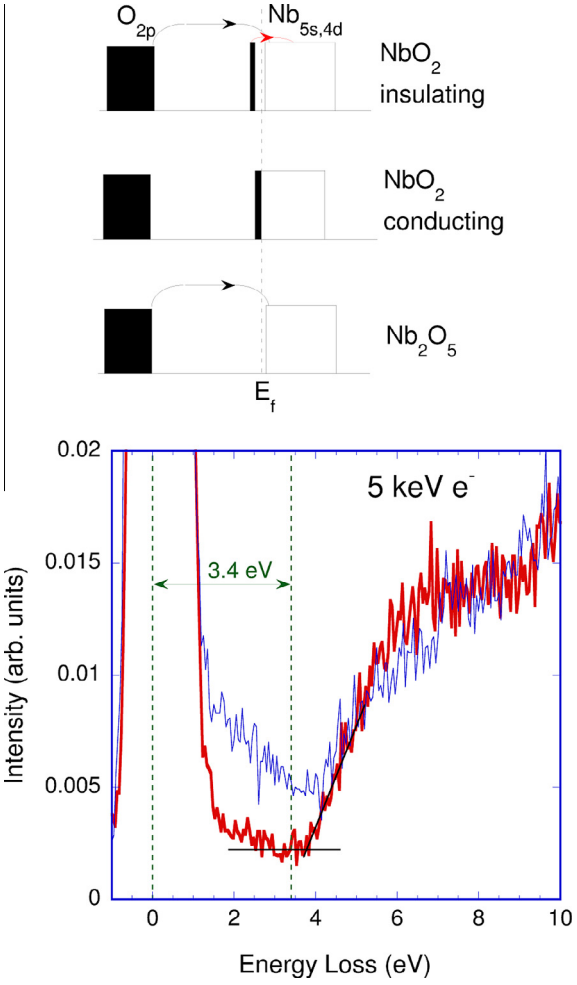

Fig. 4. Spectra taken at 5 keV for a samples grown with an $Ar:O_2$ pressure ratio of 16:4 (thick, red line) and 19:1 (thin blue line). The onset of the loss feature is estimated by the straight line extrapolation (shown in black) indicates a slightly larger band gap than usually quoted value of 3.4 for Nb_2O_5. The sample grown under low O_2 flux has a less pronounced minimum after the elastic peak. The extra intensity between 0 and 4 eV is attributed to excitation of $Nb_{4d,5s}$ electrons, as illustrated in the caricature of the density of states above the graph. (For interpretation of the references to color in this figure legend, the reader is referred to the web version of this article.)

4. Discussion and conclusion

For traditional RBS, using He^+ ions it is difficult to measure the O concentration for NbO_x films grown on Si as the weak O signal is superimposed on a background due to ions backscattered from Si at a significant depth. Therefore we made a separate set of films deposited on a carbon substrate. The gas mixtures and pressures were the same, but here the deposition was done at half the power.

Depositions using a mixture with a large O_2 content in the plasma were over-stoichiometric according to RBS, whereas ERBS values appeared to be in agreement with the Nb_2O_5 composition (see Table 1). For lower O_2 pressures the stoichiometry found with RBS and ERBS are in good agreement. Both techniques observed a strong decline in the deposition rate with increasing O_2 pressure.

In summary we have demonstrated that it is possible to characterize sputter-deposited layers such as the present NbO_x layers by electron scattering. This technique provides useful information about the stoichiometry and the thickness of the films and its electronic structure and can also determine the stoichiometry for samples that are deposited on a high-*Z* substrate. Niobium oxides can be formed by sputter-deposition that show either a threshold switching or memory switching. By simply changing the flow rates of the gases during sputter deposition one can incorporate both behaviors in a single layers. As suggested before [5,6] this could be a very economic way of overcoming sneak currents in memory devices in a simple cross bar structure. ERBS has been shown to be a good technique to monitor the quality of such material, especially if it could be integrated in an electron microscope.

Acknowledgments

This work was made possible by funding of the Australian Research Council. P.L.G. acknowledges the Brazilian agency CAPES (proc. 102209/12-3) for the financial support.

References

[1] P.L. Grande, M. Vos, D.K. Venkatachalam, S.K. Nandi, R.G. Elliman, Determination of thickness and composition of high-*k* dielectrics using high-energy electrons, Appl. Phys. Lett. 103 (2013) 071911.
[2] M. Vos, P. Grande, D. Venkatachalam, S. Nandi, R. Elliman, Oxygen self-diffusion in HfO_2 studied by electron spectroscopy, Phys. Rev. Lett. 112 (2014) 175901.
[3] M. Vos, P.L. Grande, S.K. Nandi, D.K. Venkatachalam, R.G. Elliman, A high-energy electron scattering study of the electronic structure and elemental composition of O-implanted Ta films used for the fabrication of memristor devices, J. Appl. Phys. 114 (2013) 073508.
[4] E. Linn, R. Rosezin, C.K.R. Waser, Complementary resistive switches for passive nanocrossbar memories, Nat. Mater. 9 (2010) 403.
[5] X. Liu, S.M. Sadaf, M. Son, J. Shin, J. Park, J. Lee, S. Park, H. Hwang, Diode-less bilayer oxide (WO_x–NbO_x) device for cross-point resistive memory applications, Nanotechnology 22 (2011) 475702.
[6] X. Liu, S. Sadaf, M. Son, J. Park, J. Shin, W. Lee, K. Seo, D. Lee, H. Hwang, Co-occurrence of threshold switching and memory switching in Pt–NbO_x–Pt cells for crosspoint memory applications, IEEE Electron Device Lett. 33 (2012) 236.
[7] M.D. Pickett, G. Medeiros-Ribeiro, R.S. Williams, A scalable neuristor built with Mott memristors, Nat. Mater. 12 (2) (2013) 114–117.
[8] M.D. Pickett, R.S. Williams, Phase transitions enable computational universality in neuristor-based cellular automata, Nanotechnology 24 (2013) 384002.
[9] M. Vos, M.R. Went, Effects of bonding on the energy distribution of electrons scattered elastically at high momentum transfer, Phys. Rev. B 74 (2006) 205407.
[10] M. Went, M. Vos, Rutherford backscattering using electrons as projectiles: underlying principles and possible applications, Nucl. Instr. Meth. Phys. Res. Sect. B 266 (2008) 998–1011.
[11] F. Salvat, A. Jablonski, C.J. Powell, ELSEPA dirac partial-wave calculation of elastic scattering of electrons and positrons by atoms, positive ions and molecules, Comput. Phys. Commun. 165 (2005) 157–190.
[12] P.L. Grande, M. Vos, Exploring the Barkas effect with keV-electron scattering, Phys. Rev. A 88 (2013) 052901.
[13] S. Tanuma, C.J. Powel, D.R. Penn, Calculation of electron inelastic mean free paths, Surf. Interface Anal. 20 (1993) 77–89.
[14] M. Vos, M. Went, Splitting the plasmon peak in high-energy reflection electron energy loss experiments, J. Electron Spectrosc. Relat. Phenom. 162 (2008) 1.
[15] D. Bach, R. Schneider, D. Gerthsen, J. Verbeeck, W. Sigle, Eels of niobium and stoichiometric niobium-oxide phases. Part I: Plasmon and near-edges fine structure, Microsc. Microanal. 15 (2009) 505–523.
[16] M.A. Henderson, A surface perspective on self-diffusion in rutile TiO_2, Surf. Sci. 419 (1999) 174–187.
[17] V. Eyert, The metal-insulator transition of NbO_2: an embedded peierls instability, Europhys. Lett. 58 (2002) 851.